Author Manuscript

Author Manuscript

Author Manuscript

Author Manuscript

HHS Public Access

Author manuscript

Sci Total Environ. Author manuscript; available in PMC 2023 February 25.

Published in final edited form as:

Sci Total Environ. 2022 February 25; 809: 151118. doi:10.1016/j.scitotenv.2021.151118.

Redox sensitive miR-27a/b/Nrf2 signaling in Cr(VI)-induced carcinogenesis

Lin Wang[*,1], **Khaliunaa Bayanbold**[*,1,2], **Lei Zhao**[3], **Yifang Wang**[1], **Andrea Adamcakova-Dodd**[4], **Peter S. Thorne**[4], **Hushan Yang**[3], **Bing-Hua Jiang**[#,1], **Ling-Zhi Liu**[#,3]

[1]Department of Pathology, Anatomy and Cell Biology, Thomas Jefferson University, Philadelphia, PA, United States.

[2]Department of Pathology, University of Iowa, Iowa City, IA, United States.

[3]Department of Medical Oncology, Thomas Jefferson University, Philadelphia, PA, United States.

[4]Department of Occupational and Environmental Health, University of Iowa, Iowa City, Iowa, USA.

Abstract

Hexavalent chromium [Cr(VI)] is a well-known carcinogen that can cause several types of cancer including lung cancer. NF-E2-related factor 2 (Nrf2), the redox sensitive transcription factor, can protect normal cells from a variety of toxicants and carcinogens by inducing the expression of cellular protective genes and maintaining redox balance. However, Nrf2 also protects cancer cells from radio- and chemo-therapies and facilitates cancer progression. Although Cr(VI) treatment has been demonstrated to upregulate Nrf2 expression, the mechanisms for Nrf2 regulation upon chronic Cr(VI) exposure remain to be elucidated. We found that Nrf2 was upregulated in BEAS-2B cells exposed to Cr(VI) from 1 to 5 months, and also in Cr(VI)-induced transformed (Cr-T) cells with Cr(VI) treatment for 6 months. We showed that KEAP1, the classic negative regulator of Nrf2, was downregulated after Cr(VI) exposure for 4 months, suggesting that Nrf2 induction by Cr(VI) treatment is through KEAP1 decrease at late stage. To further decipher the mechanisms of Nrf2 upregulation at early stage of Cr(VI) exposure, we demonstrated that miR-27a and miR-27b were redox sensitive miRNAs, since reactive oxygen species (ROS)

[#]To whom correspondence should be addressed: Ling-Zhi Liu. ling-zhi.liu@jefferson.edu.; Bing-Hua Jiang. Binghua.jiang@jefferson.edu.

[*]These authors contributed equally to this work.

Publisher's Disclaimer: This is a PDF file of an unedited manuscript that has been accepted for publication. As a service to our customers we are providing this early version of the manuscript. The manuscript will undergo copyediting, typesetting, and review of the resulting proof before it is published in its final form. Please note that during the production process errors may be discovered which could affect the content, and all legal disclaimers that apply to the journal pertain.

CRediT authorship contribution statement

Lin Wang: Methodology, Formal analysis, Investigation, Visualization, Writing– review & editing. **Khaliunaa Bayanbold:** Methodology, Formal analysis, Investigation, Validation, Writing– original draft. **Lei Zhao:** Methodology, Investigation. **Yifang Wang:** Methodology, Investigation. **Andrea Adamcakova-Dodd:** Methodology, Investigation. **Peter S. Thorne**: Methodology, Investigation. Writing– review & editing. **Hushan Yang:** Methodology. **Bing-Hua Jiang:** Conceptualization, Supervision, Methodology. **Ling-Zhi Liu:** Conceptualization, Supervision, Methodology, Writing– original draft, review & editing.

Conflicts of interest

The authors declare that they have no competing interests.

Declaration of interests

The authors declare that they have no known competing financial interests or personal relationships that could have appeared to influence the work reported in this paper.

Author Manuscript Author Manuscript Author Manuscript Author Manuscript

scavengers induced miR-27a/b expression. After Cr(VI) exposure for 1 month, the expression levels of miR-27a/b was dramatically decreased. The changes of miR-27a/b and their target Nrf2 were confirmed *in vivo* by mouse model intranasally exposed to Cr(VI) for 12 weeks. Nrf2 was a direct target of miR-27a/b, which acted as tumor suppressors *in vitro* and *in vivo* to inhibit tumorigenesis and cancer development of Cr-T cells. The results suggested that the inhibition of miR-27a/b was responsible for Nrf2 upregulation at both early stage and late stage of Cr(VI) exposure. This novel regulation of Nrf2 upon chronic Cr(VI) exposure through redox-regulated miR-27a/b will provide potential targets for preventing and treating Cr(VI)-induced carcinogenesis in the future.

Graphical Abstract

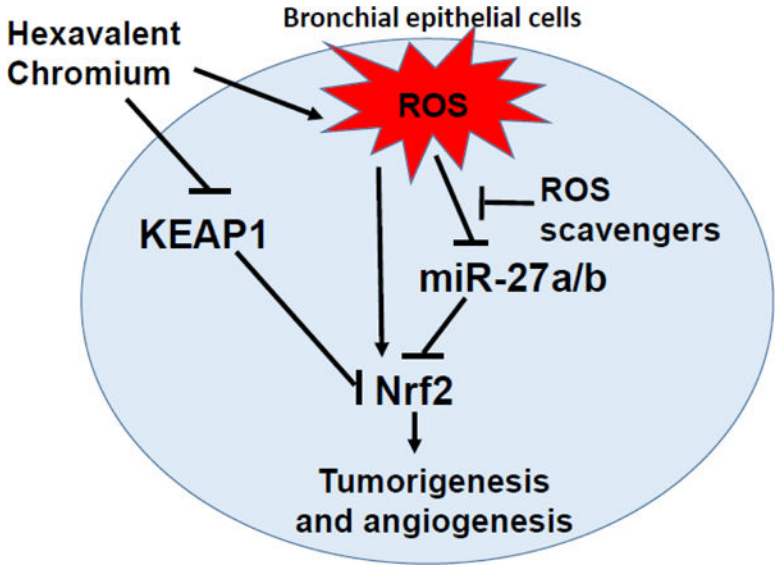

Keywords

chromium (VI); lung cancer; miR-27a/b; Nrf2; tumor growth

1. Introduction

Chromium is a steely-grey, hard and brittle transition metal. Many industries including fuel combustion (natural gas, coal, and oil) factories, chromate or chromium production and plating, stainless steel production, textile manufacturing, leather-tanning industries, pigment manufacturing, welding, polishing, and grinding, release largest amounts of chromium into the environment (Health, 2013). Two main oxidation states are commonly found in nature: trivalent chromium-Cr (III) and hexavalent chromium-Cr (VI). Cr (VI) can be absorbed into all type of cells, intracellular Cr (VI) undergoes metabolic reduction to Cr (III) by producing highly reactive intermediates Cr (V/IV) in mitochondria and microsomes. During reduction process, the molecular oxygen is reduced into superoxide ($\cdot O_2^-$) and further into hydrogen peroxide (H_2O_2) by superoxide dismutase (SOD). Moreover, reactive oxygen species (ROS) including hydroxyl radical (·OH), singlet oxygen, superoxide and hydrogen peroxide are

Author Manuscript Author Manuscript Author Manuscript Author Manuscript

produced by the Fenton-like reaction due to H_2O_2 reaction with Cr(V), Cr(IV), or Cr(III) (Wetterhahn and Hamilton, 1989). Cr(VI) is a well-known carcinogen, and chronic exposure to Cr(VI) through water, air or from landfills is associated with development of various cancers including lung cancer (Bidstrup, 1950; Keegan et al., 2008; Urbano et al., 2012). The Cr(VI) levels in welding fumes may reach as high as 1500 μg/m^3 (1.4 μM) (Pellerin and Booker, 2000). In India, Cr(VI) levels may reach up to 3.4 mg/L (65.4 μM) in surface water and 0.6 mg/L (1.154 μM) in groundwater in Sukinda valley (Das and Singh, 2011). Thus, the Cr (VI) doses used in this study is relevant to human exposure.

Cr(VI) exposure causes DNA damage, abnormal signaling transduction, alterations of epigenetic regulation such as changes of histone modifications and DNA methylations, and inflammatory responses, which are closely related to Cr(VI)-induced carcinogenesis (Carpenter and Jiang, 2013; Chen et al., 2019b; Johansen et al., 1994; Rager et al., 2019; Solano-Lopez et al., 2006; Valko et al., 2006).

Intracellular reduction of Cr(VI) leads to the ROS generation and subsequent oxidative damage to DNA, proteins and lipids, which is believed to contribute to the process of carcinogenesis. For example, ROS production during the detoxification processes leads to DNA lesions, since the interaction of DNA with Cr detoxification products, especially those that have Cr conjugated to the ROS scavengers such as GSH-Cr-DNA and Vitamin C-Cr-DNA, as well as some amino acid residues of protein such as histidine or cysteine, induces DNA double strand breaks and mutagenicity(Chen et al., 2019b; Quievryn et al., 2003; Zhitkovich, 2005). Welding fume exposure induces increased levels of oxidative stress markers and the changes DNA methylation in isolated peripheral blood mononuclear cells, as well as changes of mRNA modifications(Chen et al., 2019a; Shoeb et al., 2017). ROS generation by Cr(VI) also activates cell survival signaling pathways related with cancer initiation and tumor development(Carpenter and Jiang, 2013; Nickens et al., 2010). Overall, the ROS production and oxidative stress during intracellular Cr(VI) metabolism play important roles in Cr(VI)-induced carcinogenesis.

NF-E2-related factor 2 (Nrf2) is a redox sensitive transcription factor which regulates cellular antioxidant responses against cellular damage from oxidative stress to restore cellular redox balance, which leads to the expression of cytoprotective enzymes, such as NAD(P)H: quinone oxidoreductase 1 (NQO1) and heme oxygenase 1 (HO-1). Kelch-like ECH-associated protein 1 (KEAP1), the negative regulator of Nrf2, interacts with Nrf2 to cause its ubiquitination and proteasomal degradation under normal cellular conditions. However, under stress conditions such as ROS, exposure to electrophiles, xenobiotics, metals exposure and UV radiation, KEAP1-dependent Nrf2 ubiquitination activity is disrupted, which activates and translocates Nrf2 into the nuclei. Nrf2 is the central transcriptional regulator in antioxidant response element (ARE)-driven gene expression in response to oxidative stress (Kansanen et al., 2013; Rojo de la Vega et al., 2018). The dual roles of Nrf2 in malignant transformation and carcinogenesis has been verified: Nrf2 has protective effect before malignant transformation and during tumor initiation by maintaining redox balance upon oxidative stress, and the oncogenic effect by promoting malignant progression of cancer cells (Hammad et al., 2019; He et al., 2007; Jaramillo and Zhang, 2013; Jessen et al., 2020; Lignitto et al., 2019; Menegon et al., 2016; Satoh et al., 2013;

Author Manuscript Author Manuscript Author Manuscript Author Manuscript

Sporn and Liby, 2012). However, little information is known about Nrf2 in Cr(VI)-induced malignant transformation and carcinogenesis yet. Although recent studies have shown the important role of Nrf2/KEAP1/ARE pathway in Cr (VI)-induced toxicity and carcinogenesis (Shaw et al., 2020; Son et al., 2017), the mechanisms of Nrf2 regulation upon long-term Cr(VI) exposure remains to be elucidated.

In the present study, we found that KEAP1 was responsible for Nrf2 upregulation at late stage of Cr (VI) exposure. The suppression of a novel redox-sensitive regulatory pathway miR-27a/b/Nrf2 led to Nrf2 upregulation at both early and late stages of Cr (VI) exposure, which is a new finding of Nrf2 regulation. We verified that oxidative stress decreased miR-27a/b expression levels. Nrf2 was a direct target of miR-27a/b. miR-27a/b suppression and Nrf2 upregulation played important roles in promoting Cr-T cells-induced carcinogenesis and tumor development.

2. Materials and Methods

2.1 Cells, reagents and plasmids

Human immortalized normal bronchial epithelia cells BEAS-2B were obtained from American Type Culture Collection (ATCC) (Manassas, VA). BEAS-2B cells chronically exposed to 1μM chromium for six month to obtain Cr(VI)-transformed (Cr-T) cells, which were verified by colony formation assay *in vitro* and tumor growth assay *in vivo* (He et al., 2013; Wang et al., 2019). The passage-matched parental BEAS-2B cells were used as control cells without Cr (VI) exposure. The pair of B2B and Cr-T cells cultured in DMEM medium supplemented with 10% FBS and 1% Penicillin and Streptomycin (Life Technologies, Carlsbad, CA) under 5% CO_2 condition at 37°C. NAC, PEG-catalase, PEG-SOD, and PEG control powder were from MilliporeSigma. MiRNA negative control (miR-NC), miR-27a, and miR-27b mimics were from ThermoScientific (Rockford, IL). Lentiviral vector alone, vector containing miR-27a, miR-27b, and Nrf2 ORF without 3'-UTR were from Genecopoiea (Rockville, MD). Nrf2 expression vector pcDNA3-Myc3-Nrf2 and empty control vector pcDNA3 were from Addgene (Watertown MA). Jetprime (Polyplus) and lipofectamine3000 (Thermoscientific) transfection reagent were used according to the manufacture's instruction for transient transfection experiments.

2.2 Immunoblotting assay

For Nrf2 and KEAP1 expression in cytoplasm and nuclei, we used NE-PER Nuclear and Cytoplasmic Extraction Kit (Thermo Scientific, Rockford, IL). BEAS-2B and Cr-T cells were lysed and separated into nuclear and cytoplasmic fraction according to the manufacture's instruction. For the whole cell lysate, RIPA buffer (150 Mm NaCI, 100mM Tris pH 8.0, 1% Triton X-100, 1% deoxycholic acid, 0.1% SDS, 5mM EDTA, 10Mm NaF) containing phosphatase and protease inhibitor was used. 20–30 μg protein extracts were used for each loading and separated by 10–15% SDS-PAGE. Then proteins were transferred into PDVF membrane and blocked with 5% skim milk. Primary antibodies against Nrf2 (1:1000, Cell Signaling Technology, USA), Nrf2 (1:1000, Santa Cruz Technology, USA), HO-1 (1:1000, Santa Cruz Technology, USA), NQO1 (1:1000, Santa Cruz Technology, USA), KEAP1 (1:1000, Santa Cruz Technology, USA), GAPDH (1:1000, DSHB, USA) or β-actin

Author Manuscript Author Manuscript Author Manuscript Author Manuscript

(1:2000, Santa Cruz Technology, USA) were used to incubate the membrane overnight. After probed with corresponding secondary antibodies, protein bands were visualized using enhanced chemiluminescence system reagents (Thermo Fisher Scientific, USA) and images were developed by ChemiDoc Touch Imaging System.

2.3 Fluorescent immunohistochemical staining

For Nrf2 staining, 2000 cells of BEAS-2B and Cr-T were seeded on 8-well chambered coverglass slides (ThermoScientific) and incubated overnight at 37°C. Then, cells were fixed with 4% paraformaldehyde PBS (pH 7.4) for 10 minutes and permeabilized with 0.1% Triton X-100 for 20 minutes at RT. Cells were incubated at 4°C overnight with Nrf2 primary antibody (#12721, Cell Signaling Technology) after blocking with 1% BSA, 22.52 mg/ml glycine in PBST (PBS+0.1% Tween 20). Following day, cells were washed with PBS three times and labeled with Alexa Fluor 594-conjugated goat anti-mouse IgG secondary antibody (A-11005, Invitrogen) at RT for 1 hour. ProLong™ Diamond Antifade Mountant with DAPI (ThermoScientific Rockford, IL) was used for staining cell nuclei and mounting the samples. Fluorescence images were acquired using a Nikon DS-Ri2 and analyzed in Nikon NIS-Elements AR software.

2.4 RNA Isolation and RT-qPCR

Total RNAs were extracted with Trizol reagent (Invitrogen) according to the manufacturer's instruction. The expression levels of miR-27a and miR-27b were detected using Taqman microRNA Assay Kit (ThermoScientific, Rockford, IL). U6 small nuclear RNA was used as an internal control to normalize the expression of miR-27a and miR-27b. mRNA levels of NQO1 and HO-1 were detected using SYBR-Green RT-qPCR (Applied Biosystems, Carlsbad, CA) and GAPDH was used as an internal control. The primers used for SYBR-Green RT-qPCR were:

NQO1 forward primer: 5'-GAAGAGCACTGATCGTACTGGC-3',

NQO1 reverse primer: 5'-GGATACTGAAAGTTCGCAGGG-3';

HO-1 forward primer: 5'-AAGACTGCGTTCCTGCTCAAC-3';

HO-1 reverse primer: AAAGCCCTACAGCAACTGTCG

GAPDH forward primer: 5'-ATGGGTGTGAACCATGAGAAGTATG-3';

GAPDH reverse primer: 5'-GGTGCAGGAGGCATTGCT-3'.

2.5 Dual Luciferase reporter assay

We synthesized oligomers for wild type (WT) and mutant (Mut) Nrf2 3'-UTR with SpeI and HindIII restriction sites, then did annealing and subcloned into pMIR-reporter luciferase vector. The oligomers for Nrf2 3'-UTR were as follows (enzyme restriction sites were shown using letters with underline. Seed sequences were shown using Italy font. Bold letters showed 4-bp mutation in seed sequence, as shown in Fig. 4B):

Author Manuscript Author Manuscript Author Manuscript Author Manuscript

WT forward oligomer: 5'- CTAGTAAGCTCCT*AC**TGTG**A*TGTGAAATA −3';

WT reverse oligomer: 5'- AGCTTATTTCACA*T**CACA**GT*AGGAGCTTA −3';

Mut forward oligomer: 5'- CTAGTAAGCTCCT*AC**GTGC**A*TGTGAAATA −3';

Mut reverse oligomer: 5'- AGCTTATTTCACA*T**GCAC**GT*AGGAGCTTA −3'.

Cr-T cells were transfected with miR-27a, miR-27b mimics or miRNA negative control (miR-NC) and the luciferase reporters containing WT or Mut Nrf2 3'-UTR using Lipofectamine 3000. Cells harvested and the luciferase activity was measured using the Dual Luciferase Reporter Assay System (Promega, Madison, WI) 48 hours post transfection according to the manufacturer's instruction.

2.6 Cell proliferation assay

Cr-T cells transfected with miR-NC and miR-27a/b mimics and cell proliferation rates were detected using Methyl Thiazolyl Tetrazolium (MTT) assay. Transfected Cr-T cells were seeded into 96-well plates and cultured for 5 days. 20 μL of MTT reagent (5 mg/mL, Sigma-Aldrich, St. Louis, MO, USA) was added into the each well and incubated for 4 hours at 37°C. 100 μL of DMSO was added into each well after medium was removed and incubated for another 10 min. Absorbance of each well was measured at 590 nm using a CLARIOstar monochromator microplate reader (BMG Labtech, Cary, NC).

2.7 Soft agar colony formation assay

As a bottom layer, 6-well plates were pre-coated with 0.5% SPA (SeaPlaque Agarose from BMA, Rockland, ME) diluted in warm complete medium. As a top layer, Cr-T cells transfected with miR-NC or miR-27a/b mimics were suspended in 0.5% SPA at a cell concentration of $3x10^3$/ml and added over the bottom layer. Then cells were incubated at 37°C to allow colony formation in soft agar. Cells were fed with 0.3% SPA containing medium every 3 to 4 days. After two weeks of incubation, formed cell colonies were stained with nitro blue tetrazolium chloride (N6495 Thermo Fisher Scientific, USA) and counted using Image J Software.

2.8 Wound healing assay

miR-NC and miR-27a/b mimics transfected Cr-T cells were seeded into 6-well plate and cultured until cells reached 90% confluence. Wound was created on monolayer cell surfaces using a 200 μl sterile pipette tip. Wound healing effect was monitored and pictured at 0, 12 and 24 h time points using an inverted microscope (Nikon, Japan). Images at each time point were used to measure a migration distance.

2.9 Transwell migration assay

Cr-T cells transfected with miR-NC and miR-27a/b mimics were seeded into upper chamber of 24-well plate Corning (Kennebunk ME, USA) and incubated under starving condition with medium containing 0.1% Fetal Bovine Serum (FBS). As a chemoattractant, bottom chamber was filled with medium containing 10% FBS. Cells were allowed to migrate

Author Manuscript Author Manuscript Author Manuscript Author Manuscript

through 8.0 μm transwell pore towards the bottom chamber overnight at 37°C. Then cells were washed with cold PBS and fixed with cold 20% methanol and 3% formaldehyde. 0.2% crystal violet was used for cell staining, and non-migrated cells on the side of upper chamber were removed with cotton swab. Migrated cells on the side of bottom chamber were imaged and analyzed under the inverted microscope. The number of migrated cells of each group was counted from five randomly chosen fields and plotted on percentage scale.

2.10 Tube formation assay

Cr-T cells transfected with miR-NC and miR-27a/b mimics were cultured in medium containing 0.2% FBS for 24 h and the conditioned medium was collected. Human umbilical vein cells (HUVECs) were cultured in EBM-2 basic medium containing 0.2% FBS. After 24 h, HUVECs were harvested and suspended in EBM-2 basic medium mixed with equal amount of conditioned medium collected from each Cr-T cell group. Then, cell suspension of HUVECs was introduced into the Matrigel pre-coated 96-well plate and incubated for 6–12 h to allow tube formation at 37°C. Tube formation was monitored by microscopy and images were captured. Total tubular length was measured using Wimasis Image Analysis.

2.11 Lentivirus packaging and viral transduction

293T cells were transfected with miR-NC (CmiR0001-MR03), miR-27a (HmiR0297-MR03) and miR-27b (HmiR0145-MR03) purchased from Genecopoeia (Rockville, MD). PAX2 structural and pVSV-G envelope vectors were co-transfected with individual miRNA plasmid above to generate miR-NC, miR-27a and miR-27b lentivirus. Lentiviral soup was collected and filtered 48 h, 60 h and 72 h post transfection, and used to transduce Cr-T cells. Cr-T cells stably overexpressing miR-NC, miR-27a, and miR-27b were obtained by puromycin selection and verified using TaqMan RT-qPCR.

2.12 Tumor growth assay using nude mice

Fifteen nude mice at six-week-old (strain: 088, NU/NU) were purchased from the Charles River Laboratory (Wilmington, MA) and housed at animal facility. Mice were adjusted and acclimatized for one week prior to the implantation. Mice were randomly divided into 3 groups (n=5) for tumor growth assay using Cr-T cells stably overexpressing miR-NC, miR-27a and miR-27b. Equal number of cells ($2x10^6$ in 100 μl DMEM basal medium without FBS) were subcutaneously injected into both lower flanks of the mouse. Then, mice were maintained with standard care in the vivarium for several weeks to allow for tumor growth. When tumors reached visible size, xenografts were measured twice a week using a caliper. Tumor volume was calculated using the formula of $V=\text{Length} \times \text{Width}^2/2$. Mice were euthanized 4 weeks after implantation and tumor tissues were trimmed out, weighed, and dissected for further analysis to detect miR-27a/b by TaqMan real-time RT-PCR, and Nrf2 by immunoblotting assay. The animal studies were approved by the Institutional Animal Care and Use Committee (IACUC) at the University of Iowa and Thomas Jefferson University, and all animal care and handling procedures were performed in accordance with the Guidelines for the Care and Use of Laboratory Animals.

Author Manuscript Author Manuscript Author Manuscript Author Manuscript

2.13 Cr(VI) exposed mouse model by intranasal instillation

Mice (BALB/cJ, 6–8 wks old, The Jackson Laboratory, Bar Harbor, ME) were quarantined and acclimatized for 9 days before exposure. Zinc chromate ($ZnCrO_4$) particles were sonicated using a Qsonica homogenizer to produce particles sized from 0.5 to 5 μm and with a purity of >99.5%. The suspension was at an initial concentration of 1.0 mg/ml in sterile, pyrogen-free saline. Animals were intranasally exposed to a 50 μl dose of $ZnCrO_4$ suspension or saline once a week (Beaver et al., 2009), blood and lung tissue samples were collected after Cr(VI) exposure for 12 weeks. PBMCs were isolated using Ficoll Histopaque (MilliporeSigma) and used for RNA extraction to detect miR-27a and miR-27b. The study was approved by IACUC of the University of Iowa and Thomas Jefferson University, and all the animal care and procedures were in accordance with institution guidelines.

2.14 Immunohistochemical staining for CD31

Formalin-fixed paraffin-embedded tumor samples were used to obtain serial 5 μm sections. After antigen retrieval, monoclonal CD31 antibody (1:100) from BD Bioscience was used for the staining, and detected through streptavidin–biotin–horseradish peroxidase complex (SABC) formation. Sections incubated with preimmune IgG instead of the primary antibodies were used as a negative control. Slides were scanned under low power (×40) to determine five 'hot-spots' with the maximum number of microvessels, which were then evaluated at ×200 magnification. The number of microvessels in each field was determined and their average number was expressed as microvessel density and normalized by miR-NC control group.

2.15 Statistical analysis

At least three independent biological replicates have been performed to obtain all results. Results were presented as mean ± SE from independent experiments and analyzed using GraphPad Prism software. Comparison of two sets of unpaired data was performed by unpaired *t* test. A one-way analysis of variance (ANOVA) was used for the data comparison among multiple groups. A value of $p < 0.05$ indicated significant difference.

3. Results and Discussion

3.1 Nrf2 was upregulated in Cr(VI)-induced transformed (Cr-T) cells.

BEAS-2B were repetitively treated with 1 μM of Cr(VI) up to 24 weeks. The passage-matched normal cells without Cr(VI) exposure were used as control (He et al., 2013). BEAS-2B cells are widely used in the studies of metal-induced carcinogenesis, transformation in particular, by various groups (Cai et al., 2011; Chen et al., 2010; O'Hara et al., 2007; Sun et al., 2011; Wang et al., 2011). We picked up seven single colonies from Cr-T cells treated with Cr(VI) at 1 μM for 6 months, and found out that the expression level of Nrf2 in all the colonies were upregulated (Fig. 1A). Consistent with this result, Cr-T cells possessed higher expression of Nrf2, especially in nuclei (Fig. 1B and C). Compare to parental BEAS-2B cells where Nrf2 mainly located in cytoplasm, the expression of Nrf2 in Cr-T cells were translocated into nuclei (Fig. 1D). Correspondingly, NQO1 and HO-1, the downstream targets of Nrf2, were upregulated in cells treated with Cr(VI) for 1, 2, and 3

Author Manuscript Author Manuscript Author Manuscript Author Manuscript

months (Fig. 1E and F). Overall, the results indicate that chronic exposure to low dose of Cr(VI) results in Nrf2 upregulation in immortalized normal human bronchial epithelial cells.

Cr(VI) is an environmental carcinogen that causes different types of cancer, such as lung, gastrointestinal, pancreas, prostate, bladder cancer and cancer of the paranasal sinuses and nasal cavity. Although abnormal signaling transduction, alteration of epigenetic regulation and inflammatory responses have been reported in response to Cr(VI) exposure(Kart et al., 2016; Wang et al., 2016; Zuo et al., 2012), there remains a critical need to investigate the mechanism underlying Cr(VI)-induced carcinogenesis for better disease prevention. We and other researchers have demonstrated that metal-promoted ROS generation and the activation of oxidative stress signaling pathways play important roles in metal-induced carcinogenesis and tumor development (Azad et al., 2008; Caglieri et al., 2008; Carpenter et al., 2011; Harris and Shi, 2003; He et al., 2014; Jing et al., 2012; Liu et al., 2015; Liu et al., 2011). Consistent with Cr(VI)-induced ROS production, the redox sensitive Nrf2 was upregulated to activate cellular antioxidant responses to restore cellular redox balance.

3.2 Downregulation of KEAP1 was responsible for increased Nrf2 expression at late stage, but not at early stage of Cr(VI) exposure.

In our study, we found that long-term exposure of Cr(VI) caused immortalized human bronchial epithelial BEAS-2B cells to undergo malignant transformation (He et al., 2013; Wang et al., 2019). It has been well known that Nrf2 has dual roles in carcinogenesis: Nrf2 is considered as a tumor suppressor under normal cellular regulations through preventing cancer initiation by reducing redox induction. However, after malignant transformation of cells, Nrf2 has been demonstrated to promote cancer cell proliferation, invasion and treatment resistance to chemo- or radio-therapy, which further results in cancer progression (Cloer et al., 2019; He et al., 2020; Jaramillo and Zhang, 2013). Oxidative stress disrupts KEAP1-dependent Nrf2 ubiquitination activity and activates Nrf2 to translocate into the nuclei, thus transcriptionally promoting the expression of its downstream antioxidants and detoxifying enzymes. In order to study the mechanism of Nrf2 overexpression in Cr-T cells, we detected expression level of KEAP1, the classical negative regulator of Nrf2. As shown in Fig. 2A and B, Cr-T cells possessed lower levels of KEAP1, decrease of KEAP1 occurred in both cytoplasm and nuclei, especially in nuclei. Intriguingly, we found that Nrf2 and its downstream molecules NQO1 and HO-1 were upregulated at the protein level after Cr(VI) treatment of BEAS-2B cells for 1, 2, 3, 4 and 5 month. However, KEAP1 downregulation was only exhibited after treatment for 4 and 5 months, but not at early stage at 1, 2 and 3 months (Fig. 2C), suggesting that in addition to classical KEAP1/Nrf2 regulation, there must be other molecular mechanisms for Nrf2 upregulation upon chronic Cr(VI) treatment at early stage.

3.3 miR-27a and miR-27b were downregulated upon long-term Cr(VI) exposure *in vitro* and *in vivo*.

MicroRNAs are small single stranded non-coding RNA molecules approximately 18–24 nucleotides in length found in all eukaryotic cells, which have a role in mediating post-transcriptional regulation and almost all biological pathways (Filipowicz et al., 2008). It has been reported that over 60% of human genes are directly regulated by microRNAs

Author Manuscript Author Manuscript Author Manuscript Author Manuscript

(Friedman et al., 2009). They are involved in important cellular biogenesis such as cell cycle control, proliferation, metabolism, cell differentiation and development, and apoptosis (Lin and Gregory, 2015; Treiber et al., 2019). Dependent their function, miRNAs serve as oncogenes and tumor suppressors (Lee and Dutta, 2009; Rupaimoole and Slack, 2017). However, the role and mechanisms of miRNAs in Cr(VI)-induced carcinogenesis remain to be elucidated. Our previous miRNA array data using parental BEAS-2B and Cr-T cells showed downregulation of miR-27a/b in Cr-T cells. Consistent with the array results, we found that expression levels of miR-27a and miR-27b were significantly suppressed in Cr(VI)-treated cells in a time-dependent manner for 1–3 months (Fig. 3B), and in Cr-T cells exposed Cr(VI) for 6 months (Fig. 3A). More importantly, BALB/cJ mice were exposed to $ZnCrO_4$ suspension at a concentration of 1.0 mg/ml for 12 weeks as previously described (Beaver et al., 2009). We found that compared to control, peripheral blood mononuclear cells (PBMCs) in blood samples from Cr(VI)-exposed mice for 12 weeks had lower levels of miR-27a/b (Fig. 3C). Similarly, lung tissues from Cr(VI)-exposed mice also showed significant downregulation of miR-27a and miR-27b by TaqMan real-time PCR assay (Fig. 3D). In addition, the results in lung tissues suggested an inverse correlation between miR-27a/b and Nrf2 expression (Fig. 3E, $r=-0.643$ and $r=-0.394$, respectively). Thus, in the present study, we revealed a novel mechanism by which Cr(VI) exposure caused Nrf2 upregulation during early stage through miR-27a/b downregulation.

3.4 miR-27a/b directly targeted Nrf2.

By using TargetScan and miRDB target prediction software, miR-27a/b may directly target Nrf2 (Fig. 4A). We made wild type reporter containing 3'-UTR of Nrf2 and mutant reporter with 4 bp mutation (Fig. 4B). Luciferase assay showed that overexpression of either miR-27a or miR-27b markedly suppressed wild type, but not mutant reporter activity (Fig. 4C), suggesting that miR-27a/b binds to the seed sequence of Nrf2 to inhibit its expression. Furthermore, overexpression of anti-miR-27a/b inhibitors in parental BEAS-2B cells increased, while overexpression of miR-27a/b mimics in Cr-T cells decreased Nrf2 expression, confirming that Nrf2 is a direct target of both miR-27a and miR-27b (Fig. 4D).

Some miRNAs have been reported to regulate Nrf2 expression. For example, miR-200a, miR-141, and miR-432 target KEAP1 and promote its degradation, resulting in Nrf2 activation (Akdemir et al., 2017; Cheng et al., 2017; Hu et al., 2019). Some miRNAs directly target Nrf2 to decrease its expression, including miR-365–1, miR-193b, miR-28, miR-93, miR-153, miR-27a, miR-142–5p, miR-144, miR-340, and miR-34a (Ayers et al., 2015; Zimta et al., 2019). Several studies have determined the alteration in mRNA expression profiles upon Cr(VI)-exposure (Amrani et al., 2020; Bollati et al., 2010; Chandra et al., 2015; Jia et al., 2020). Although it has been demonstrated that Nrf2 is one of targets of miR-27a/b (Song et al., 2018; Teimouri et al., 2020; Xu et al., 2017), little information is known about the role and mechanisms of miR-27a and miR-27b in long-term Cr(VI) exposure-induced carcinogenesis. In the following studies, we will further investigate the role and mechanisms of miR-27a/b and their target Nrf2 in Cr(VI)-induced carcinogenesis.

Author Manuscript Author Manuscript Author Manuscript Author Manuscript

3.5 ROS-scavengers suppressed Nrf2 expression and restored miR-27a and miR-27b expression in Cr-T cells.

Since Nrf2 is a critical redox-sensitive transcription factor to mediate homeostasis, we sought to determine whether oxidative stress regulates miR-27a/b expression. We found that ROS scavengers 5 mM NAC treatment for 24 h and 48 h markedly suppressed Nrf2 protein expression (Fig. 5A), SOD1 and catalase treatment for 24 h dramatically inhibited Nrf2 expression (Fig. 5B and C). On the contrary, NAC treatment induced miR-27a expression after 48 h, and increased miR-27b expression after 24 and 48 h (Fig. 5D). Similarly, PEG-SOD1 and PEG-catalase treatment for 24 h significantly increased miR-27a/b expression levels (Fig. 5E and F). In summary, the results have demonstrated that miR-27a/b are redox sensitive miRNAs, and inhibition of ROS generation can suppress Nrf2 level partially through miR-27a/b upregulation. Redox sensitive miR-27a/b/Nrf2 pathway is a novel mechanism in Cr(VI)-induced Nrf2 upregulation.

3.6 MiR-27a/b acted as tumor suppressors in Cr-T cells to inhibit cell proliferation, colony formation, migration and tube formation *in vitro*.

Next, we asked what are the biological functions of miR-27a/b? Cancer cell proliferation, colony formation, migration, tube formation and tumor growth are vital process for cancer initiation and development. We overexpressed miR-27a and miR-27b by transient transfection with miRNA mimics (miR-27a and miR-27b) to 150- and 200-fold in Cr-T cells, respectively. Cells transfected with negative control of miRNA (miR-NC) in Cr-T cells were used as negative control (Fig. 6A). Overexpression of miR-27a/b significantly reduced cell proliferation rate (Fig. 6A), decreased the number of colonies formed (Fig. 6B), inhibited cell migration by wound healing and trans-well migration assays (Fig. 6C and D), and suppressed tube formation (Fig. 6E), suggesting the antitumor role of miR-27a/b in Cr-T cells *in vitro*.

3.7 MiR-27a/b inhibited Cr-T cells-induced tumor growth and angiogenesis in nude mice.

Furthermore, in order to study the antitumor function of miR-27a/b *in vivo*, we established miR-27a and miR-27b overexpression stable cell lines using Cr-T cells by lentiviral transduction and puromycin selection (Fig. 7A). Tumor growth assay showed that compared to control group, miR-27a and miR-27b groups showed smaller tumor size and less tumor formation (Fig. 7B and C). In miR-NC control group, 9 out of 10 injections formed tumor, whereas 3 out of 10 implantations formed tumor in miR-27a group, suggesting that forced expression of miR-27a in Cr-T cells significantly inhibited tumor initiation. In miR-27b group, 8 out of 10 injections formed tumors, but in smaller size, indicating that overexpression of miR-27b suppressed tumor growth of Cr-T cells (Fig. 7B and C, Table 1). Forced expression of miR-27a/b decreased tumor weight (Fig. 7D). Moreover, the expression levels of miR-27a and miR-27b from xenografts in Cr-T cells stably overexpressing miR-27a/b groups were higher than those from xenografts in control group (Fig. 7E). Forced expression miR-27a/b inhibited Nrf2 expression in tumor samples (Fig. 7F). We also found that compared to miR-NC groups, miR-27a/b overexpression suppressed angiogenesis to less than 50%, showing fewer CD31 positive microvessels (Fig. 7G). The

Author Manuscript Author Manuscript Author Manuscript Author Manuscript

results reveal that miR-27a/b play important roles as tumor suppressors by targeting Nrf2 in Cr-T induced tumor formation, tumor growth and angiogenesis *in vivo*.

3.8 Forced expression of Nrf2 restored miR-27a/b-inhibited cell proliferation, colony formation, migration and tube formation.

In order to determine whether miR-27a/b exert their function through Nrf2, we overexpressed miR-27a/b with or without Nrf2 expression (Fig. 8A), then test cell proliferation, colony formation, migration, and tube formation. The results showed that forced expression of Nrf2 recovered miR-27a/b-inhibited cell proliferation (Fig. 8B), colony formation (Fig. 8C), cell migration (Fig. 8D), and tube formation (Fig. 8E). These results suggest that in Cr-T cells, miR-27a/b exhibit tumor suppressor role by targeting Nrf2 to suppress the biological processes of cancer development.

4. Conclusions

Cr(VI) is a well-known carcinogen to cause lung cancer by DNA double-strand breaks, ROS generation, epigenetic regulation, and inflammatory responses. In this study, we investigated molecular mechanism of Cr(VI)-induced cell transformation and carcinogenesis, and found that long-term exposure to Cr(VI) resulted in dramatic downregulation of tumor suppressor-like miR-27a/b by more than 100-fold. ROS scavengers restored the expression levels of miR-27a/b and inhibited Nrf2 expression. These new redox-sensitive miRNAs were responsible for Nrf2 upregulation during early stage of Cr(VI) exposure from 1 month to 3 months, revealing a novel molecular mechanism of Cr(VI)-induced Nrf2 regulation. At late stage of Cr(VI) treatment from 4 months to 6 months, both miR-27a/b/Nrf2 and KEAP1/Nrf2 pathways were involved in mediating the upregulation of Nrf2 expression. MiR-27a/b acted as tumor suppressors to attenuate Cr-T cell proliferation, colony formation, migration, tube formation, and tumor growth through their common target Nrf2.

Acknowledgements

This work was supported by the National Institutes of Health grants (no. R01ES027901, R01CA232587, and K02ES029119), American Cancer Society Research Scholar (no. NEC-129306), and the Environmental Health Sciences Research Center (NIH P30ES005605) at the University of Iowa, and Commonwealth University Research Enhancement Program grant with the Pennsylvania Department of Health (SAP# 4100088563).

Abbreviations:

Cr(VI)	Hexavalent chromium
Nrf2	NF-E2-related factor 2
KEAP1	Kelch-like ECH-associated protein 1
ROS	reactive oxygen species
NQO1	NAD(P)H: quinone oxidoreductase 1
HO-1	heme oxygenase 1
ARE	antioxidant response element

Author Manuscript Author Manuscript Author Manuscript Author Manuscript

Cr-T cells	Cr(VI)-transformed cells

References

Akdemir B, Nakajima Y, Inazawa J, Inoue J. miR-432 Induces NRF2 Stabilization by Directly Targeting KEAP1. Mol Cancer Res 2017; 15: 1570–1578. [PubMed: 28760781]

Amrani I, Haddam N, Garat A, Allorge D, Zerimech F, Schraen S, et al. Exposure to metal fumes and circulating miRNAs in Algerian welders. Int Arch Occup Environ Health 2020; 93: 553–561. [PubMed: 31872268]

Ayers D, Baron B, Hunter T. miRNA Influences in NRF2 Pathway Interactions within Cancer Models. J Nucleic Acids 2015; 2015: 143636. [PubMed: 26345522]

Azad N, Iyer AK, Manosroi A, Wang L, Rojanasakul Y. Superoxide-mediated proteasomal degradation of Bcl-2 determines cell susceptibility to Cr(VI)-induced apoptosis. Carcinogenesis 2008; 29: 1538–45. [PubMed: 18544562]

Beaver LM, Stemmy EJ, Schwartz AM, Damsker JM, Constant SL, Ceryak SM, et al. Lung inflammation, injury, and proliferative response after repetitive particulate hexavalent chromium exposure. Environ Health Perspect 2009; 117: 1896–902. [PubMed: 20049209]

Bidstrup PL. Cancer of the lung in nickel, arsenic and chromate workers. Arch Belg Med Soc 1950; 8: 500–6. [PubMed: 14790766]

Bollati V, Marinelli B, Apostoli P, Bonzini M, Nordio F, Hoxha M, et al. Exposure to metal-rich particulate matter modifies the expression of candidate microRNAs in peripheral blood leukocytes. Environ Health Perspect 2010; 118: 763–8. [PubMed: 20061215]

Caglieri A, Goldoni M, De Palma G, Mozzoni P, Gemma S, Vichi S, et al. Exposure to low levels of hexavalent chromium: target doses and comparative effects on two human pulmonary cell lines. Acta Biomed 2008; 79 Suppl 1: 104–15. [PubMed: 18924316]

Cai T, Li X, Ding J, Luo W, Li J, Huang C. A cross-talk between NFAT and NF-kappaB pathways is crucial for nickel-induced COX-2 expression in Beas-2B cells. Curr Cancer Drug Targets 2011; 11: 548–59. [PubMed: 21486220]

Carpenter RL, Jiang BH. Roles of EGFR, PI3K, AKT, and mTOR in heavy metal-induced cancer. Curr Cancer Drug Targets 2013; 13: 252–66. [PubMed: 23297824]

Carpenter RL, Jiang Y, Jing Y, He J, Rojanasakul Y, Liu LZ, et al. Arsenite induces cell transformation by reactive oxygen species, AKT, ERK1/2, and p70S6K1. Biochem Biophys Res Commun 2011; 414: 533–8. [PubMed: 21971544]

Chandra S, Pandey A, Chowdhuri DK. MiRNA profiling provides insights on adverse effects of Cr(VI) in the midgut tissues of Drosophila melanogaster. J Hazard Mater 2015; 283: 558–67. [PubMed: 25464296]

Chen B, Xiong J, Ding JH, Yuan BF, Feng YQ. Analysis of the Effects of Cr(VI) Exposure on mRNA Modifications. Chem Res Toxicol 2019a; 32: 2078–2085. [PubMed: 31433169]

Chen H, Kluz T, Zhang R, Costa M. Hypoxia and nickel inhibit histone demethylase JMJD1A and repress Spry2 expression in human bronchial epithelial BEAS-2B cells. Carcinogenesis 2010; 31: 2136–44. [PubMed: 20881000]

Chen QY, DesMarais T, Costa M. Metals and Mechanisms of Carcinogenesis. Annu Rev Pharmacol Toxicol 2019b; 59: 537–554. [PubMed: 30625284]

Cheng LB, Li KR, Yi N, Li XM, Wang F, Xue B, et al. miRNA-141 attenuates UV-induced oxidative stress via activating Keap1-Nrf2 signaling in human retinal pigment epithelium cells and retinal ganglion cells. Oncotarget 2017; 8: 13186–13194. [PubMed: 28061435]

Cloer EW, Goldfarb D, Schrank TP, Weissman BE, Major MB. NRF2 Activation in Cancer: From DNA to Protein. Cancer Res 2019; 79: 889–898. [PubMed: 30760522]

Das AP, Singh S. Occupational health assessment of chromite toxicity among Indian miners. Indian J Occup Environ Med 2011; 15: 6–13. [PubMed: 21808494]

Filipowicz W, Bhattacharyya SN, Sonenberg N. Mechanisms of post-transcriptional regulation by microRNAs: are the answers in sight? Nature Reviews Genetics 2008; 9: 102.

Author Manuscript Author Manuscript Author Manuscript Author Manuscript

Friedman RC, Farh KK, Burge CB, Bartel DP. Most mammalian mRNAs are conserved targets of microRNAs. Genome Res 2009; 19: 92–105. [PubMed: 18955434]

Hammad A, Namani A, Elshaer M, Wang XJ, Tang X. "NRF2 addiction" in lung cancer cells and its impact on cancer therapy. Cancer Lett 2019; 467: 40–49. [PubMed: 31574294]

Harris GK, Shi X. Signaling by carcinogenic metals and metal-induced reactive oxygen species. Mutat Res 2003; 533: 183–200. [PubMed: 14643420]

He F, Antonucci L, Karin M. NRF2 as a regulator of cell metabolism and inflammation in cancer. Carcinogenesis 2020; 41: 405–416. [PubMed: 32347301]

He J, Qian X, Carpenter R, Xu Q, Wang L, Qi Y, et al. Repression of miR-143 mediates Cr (VI)-induced tumor angiogenesis via IGF-IR/IRS1/ERK/IL-8 pathway. Toxicol Sci 2013; 134: 26–38. [PubMed: 23748240]

He J, Wang M, Jiang Y, Chen Q, Xu S, Xu Q, et al. Chronic arsenic exposure and angiogenesis in human bronchial epithelial cells via the ROS/miR-199a-5p/HIF-1alpha/COX-2 pathway. Environ Health Perspect 2014; 122: 255–61. [PubMed: 24413338]

He X, Lin GX, Chen MG, Zhang JX, Ma Q. Protection against chromium (VI)-induced oxidative stress and apoptosis by Nrf2. Recruiting Nrf2 into the nucleus and disrupting the nuclear Nrf2/Keap1 association. Toxicol Sci 2007; 98: 298–309. [PubMed: 17420218]

Health NIfOSa. Occupational exposure to hexavalent chromium 2013.

Hu X, Liu H, Wang Z, Hu Z, Li L. miR-200a Attenuated Doxorubicin-Induced Cardiotoxicity through Upregulation of Nrf2 in Mice. Oxid Med Cell Longev 2019; 2019: 1512326. [PubMed: 31781322]

Jaramillo MC, Zhang DD. The emerging role of the Nrf2-Keap1 signaling pathway in cancer. Genes Dev 2013; 27: 2179–91. [PubMed: 24142871]

Jessen C, Kress JKC, Baluapuri A, Hufnagel A, Schmitz W, Kneitz S, et al. The transcription factor NRF2 enhances melanoma malignancy by blocking differentiation and inducing COX2 expression. Oncogene 2020; 39: 6841–6855. [PubMed: 32978520]

Jia J, Li T, Yao C, Chen J, Feng L, Jiang Z, et al. Circulating differential miRNAs profiling and expression in hexavalent chromium exposed electroplating workers. Chemosphere 2020; 260: 127546. [PubMed: 32758765]

Jing Y, Liu LZ, Jiang Y, Zhu Y, Guo NL, Barnett J, et al. Cadmium increases HIF-1 and VEGF expression through ROS, ERK, and AKT signaling pathways and induces malignant transformation of human bronchial epithelial cells. Toxicol Sci 2012; 125: 10–9. [PubMed: 21984483]

Johansen M, Overgaard E, Toft A. Severe chronic inflammation of the mucous membranes in the eyes and upper respiratory tract due to work-related exposure to hexavalent chromium. J Laryngol Otol 1994; 108: 591–2. [PubMed: 7930899]

Kansanen E, Kuosmanen SM, Leinonen H, Levonen AL. The Keap1-Nrf2 pathway: Mechanisms of activation and dysregulation in cancer. Redox Biol 2013; 1: 45–9. [PubMed: 24024136]

Kart A, Koc E, Dalginli KY, Gulmez C, Sertcelik M, Atakisi O. The Therapeutic Role of Glutathione in Oxidative Stress and Oxidative DNA Damage Caused by Hexavalent Chromium. Biol Trace Elem Res 2016; 174: 387–391. [PubMed: 27165098]

Keegan GM, Learmonth ID, Case CP. A systematic comparison of the actual, potential, and theoretical health effects of cobalt and chromium exposures from industry and surgical implants. Crit Rev Toxicol 2008; 38: 645–74. [PubMed: 18720105]

Lee YS, Dutta A. MicroRNAs in cancer. Annu Rev Pathol 2009; 4: 199–227. [PubMed: 18817506]

Lignitto L, LeBoeuf SE, Homer H, Jiang S, Askenazi M, Karakousi TR, et al. Nrf2 Activation Promotes Lung Cancer Metastasis by Inhibiting the Degradation of Bach1. Cell 2019; 178: 316–329 e18. [PubMed: 31257023]

Lin S, Gregory RI. MicroRNA biogenesis pathways in cancer. Nature Reviews Cancer 2015; 15: 321. [PubMed: 25998712]

Liu LZ, Ding M, Zheng JZ, Zhu Y, Fenderson BA, Li B, et al. Tungsten Carbide-Cobalt Nanoparticles Induce Reactive Oxygen Species, AKT, ERK, AP-1, NF-kappaB, VEGF, and Angiogenesis. Biol Trace Elem Res 2015; 166: 57–65. [PubMed: 25893364]

Liu LZ, Jiang Y, Carpenter RL, Jing Y, Peiper SC, Jiang BH. Role and mechanism of arsenic in regulating angiogenesis. PLoS One 2011; 6: e20858. [PubMed: 21687637]

Author Manuscript Author Manuscript Author Manuscript Author Manuscript

Menegon S, Columbano A, Giordano S. The Dual Roles of NRF2 in Cancer. Trends Mol Med 2016; 22: 578–593. [PubMed: 27263465]

Nickens KP, Patierno SR, Ceryak S. Chromium genotoxicity: A double-edged sword. Chem Biol Interact 2010; 188: 276–88. [PubMed: 20430016]

O'Hara KA, Vaghjiani RJ, Nemec AA, Klei LR, Barchowsky A. Cr(VI)-stimulated STAT3 tyrosine phosphorylation and nuclear translocation in human airway epithelial cells requires Lck. Biochem J 2007; 402: 261–9. [PubMed: 17078813]

Pellerin C, Booker SM. Reflections on hexavalent chromium: health hazards of an industrial heavyweight. Environ Health Perspect 2000; 108: A402–7. [PubMed: 11017901]

Quievryn G, Peterson E, Messer J, Zhitkovich A. Genotoxicity and mutagenicity of chromium(VI)/ascorbate-generated DNA adducts in human and bacterial cells. Biochemistry 2003; 42: 1062–70. [PubMed: 12549927]

Rager JE, Suh M, Chappell GA, Thompson CM, Proctor DM. Review of transcriptomic responses to hexavalent chromium exposure in lung cells supports a role of epigenetic mediators in carcinogenesis. Toxicol Lett 2019; 305: 40–50. [PubMed: 30690063]

Rojo de la Vega M, Chapman E, Zhang DD. NRF2 and the Hallmarks of Cancer. Cancer Cell 2018; 34: 21–43. [PubMed: 29731393]

Rupaimoole R, Slack FJ. MicroRNA therapeutics: towards a new era for the management of cancer and other diseases. Nat Rev Drug Discov 2017; 16: 203–222. [PubMed: 28209991]

Satoh H, Moriguchi T, Takai J, Ebina M, Yamamoto M. Nrf2 prevents initiation but accelerates progression through the Kras signaling pathway during lung carcinogenesis. Cancer Res 2013; 73: 4158–68. [PubMed: 23610445]

Shaw P, Sen A, Mondal P, Dey Bhowmik A, Rath J, Chattopadhyay A. Shinorine ameliorates chromium induced toxicity in zebrafish hepatocytes through the facultative activation of Nrf2-Keap1-ARE pathway. Aquat Toxicol 2020; 228: 105622. [PubMed: 32947073]

Shoeb M, Kodali VK, Farris BY, Bishop LM, Meighan TG, Salmen R, et al. Oxidative Stress, DNA Methylation, and Telomere Length Changes in Peripheral Blood Mononuclear Cells after Pulmonary Exposure to Metal-Rich Welding Nanoparticles. NanoImpact 2017; 5: 61–69. [PubMed: 30734006]

Solano-Lopez C, Zeidler-Erdely PC, Hubbs AF, Reynolds SH, Roberts JR, Taylor MD, et al. Welding fume exposure and associated inflammatory and hyperplastic changes in the lungs of tumor susceptible a/j mice. Toxicol Pathol 2006; 34: 364–72. [PubMed: 16844664]

Son YO, Pratheeshkumar P, Wang Y, Kim D, Zhang Z, Shi X. Protection from Cr(VI)-induced malignant cell transformation and tumorigenesis of Cr(VI)-transformed cells by luteolin through Nrf2 signaling. Toxicol Appl Pharmacol 2017; 331: 24–32. [PubMed: 28416455]

Song J, Zhang H, Sun Y, Guo R, Zhong D, Xu R, et al. Omentin-1 protects renal function of mice with type 2 diabetic nephropathy via regulating miR-27a-Nrf2/Keap1 axis. Biomed Pharmacother 2018; 107: 440–446. [PubMed: 30103116]

Sporn MB, Liby KT. NRF2 and cancer: the good, the bad and the importance of context. Nat Rev Cancer 2012; 12: 564–71. [PubMed: 22810811]

Sun H, Clancy HA, Kluz T, Zavadil J, Costa M. Comparison of gene expression profiles in chromate transformed BEAS-2B cells. PLoS One 2011; 6: e17982. [PubMed: 21437242]

Teimouri M, Hosseini H, Shabani M, Koushki M, Noorbakhsh F, Meshkani R. Inhibiting miR-27a and miR-142–5p attenuate nonalcoholic fatty liver disease by regulating Nrf2 signaling pathway. IUBMB Life 2020; 72: 361–372. [PubMed: 31889412]

Treiber T, Treiber N, Meister G. Regulation of microRNA biogenesis and its crosstalk with other cellular pathways. Nature Reviews Molecular Cell Biology 2019; 20: 5–20. [PubMed: 30228348]

Urbano AM, Ferreira LM, Alpoim MC. Molecular and cellular mechanisms of hexavalent chromium-induced lung cancer: an updated perspective. Curr Drug Metab 2012; 13: 284–305. [PubMed: 22455553]

Valko M, Rhodes CJ, Moncol J, Izakovic M, Mazur M. Free radicals, metals and antioxidants in oxidative stress-induced cancer. Chem Biol Interact 2006; 160: 1–40. [PubMed: 16430879]

Author Manuscript Author Manuscript Author Manuscript Author Manuscript

Wang L, Qiu JG, He J, Liu WJ, Ge X, Zhou FM, et al. Suppression of miR-143 contributes to overexpression of IL-6, HIF-1alpha and NF-kappaB p65 in Cr(VI)-induced human exposure and tumor growth. Toxicol Appl Pharmacol 2019; 378: 114603. [PubMed: 31152816]

Wang X, Son YO, Chang Q, Sun L, Hitron JA, Budhraja A, et al. NADPH oxidase activation is required in reactive oxygen species generation and cell transformation induced by hexavalent chromium. Toxicol Sci 2011; 123: 399–410. [PubMed: 21742780]

Wang Y, Wu W, Yao C, Lou J, Chen R, Jin L, et al. Elevated tissue Cr levels, increased plasma oxidative markers, and global hypomethylation of blood DNA in male Sprague-Dawley rats exposed to potassium dichromate in drinking water. Environ Toxicol 2016; 31: 1080–90. [PubMed: 25846368]

Wetterhahn KE, Hamilton JW. Molecular basis of hexavalent chromium carcinogenicity: effect on gene expression. Sci Total Environ 1989; 86: 113–29. [PubMed: 2602931]

Xu W, Li F, Liu Z, Xu Z, Sun B, Cao J, et al. MicroRNA-27b inhibition promotes Nrf2/ARE pathway activation and alleviates intracerebral hemorrhage-induced brain injury. Oncotarget 2017; 8: 70669–70684. [PubMed: 29050310]

Zhitkovich A Importance of chromium-DNA adducts in mutagenicity and toxicity of chromium(VI). Chem Res Toxicol 2005; 18: 3–11. [PubMed: 15651842]

Zimta AA, Cenariu D, Irimie A, Magdo L, Nabavi SM, Atanasov AG, et al. The Role of Nrf2 Activity in Cancer Development and Progression. Cancers (Basel) 2019; 11.

Zuo Z, Cai T, Li J, Zhang D, Yu Y, Huang C. Hexavalent chromium Cr(VI) up-regulates COX-2 expression through an NFkappaB/c-Jun/AP-1-dependent pathway. Environ Health Perspect 2012; 120: 547–53. [PubMed: 22472290]

Author Manuscript Author Manuscript Author Manuscript Author Manuscript

Highlights

- MiR-27a and miR-27b are novel oxidative stress-regulated miRNAs.
- MiR-27a/b suppression leads to Nrf2 upregulation upon Cr(VI) exposure.
- KEAP1 is responsible for Nrf2 upregulation at late stage of Cr(VI) exposure.
- MiR-27a/b are tumor suppressors to inhibit carcinogenesis by direct targeting Nrf2.

Author Manuscript Author Manuscript Author Manuscript Author Manuscript

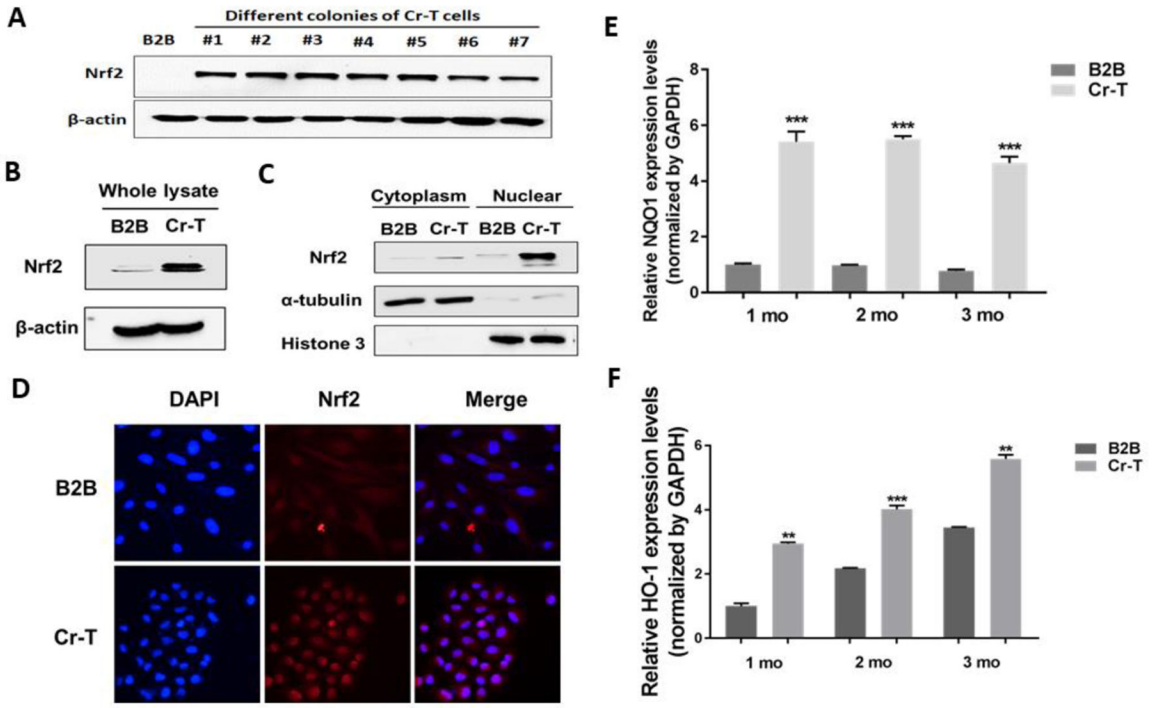

Fig. 1. Nrf2 was upregulated in Cr-T cells.

(**A**) BEAS-2B cells were treated with 1 μM of Cr(VI) for 6 months. These Cr-T cells were transformed and formed colonies *in vitro* and tumor *in vivo*. Single colonies were isolated from Cr-T cells above. Passage matched parental BEAS-2B (B2B) cells were used as control. The expression levels of Nrf2 and β-actin were determined using immunoblotting assay in 7 different Cr-T colonies. (**B**) Nrf2 and β-actin expression in pooled Cr-T cells. (**C**) The expression of Nrf2 in cytoplasm and nuclear fraction. α-tubulin and Histone 3 were used as an internal control for cytoplasm and nuclear fraction, respectively. (**D**) Immunofluorescence staining for Nrf2 (red) and DAPI (blue). Magnification: 400x. (**E** and **F**) BEAS-2B cells were treated with 1 μM of Cr(VI) for 1, 2 and 3 months. The mRNA levels of NQO1 and HO-1 were measured using real-time PCR. **, $p < 0.01$ compared to parental B2B cells. ***, $p < 0.001$ compared to parental B2B cells.

Author Manuscript Author Manuscript Author Manuscript Author Manuscript

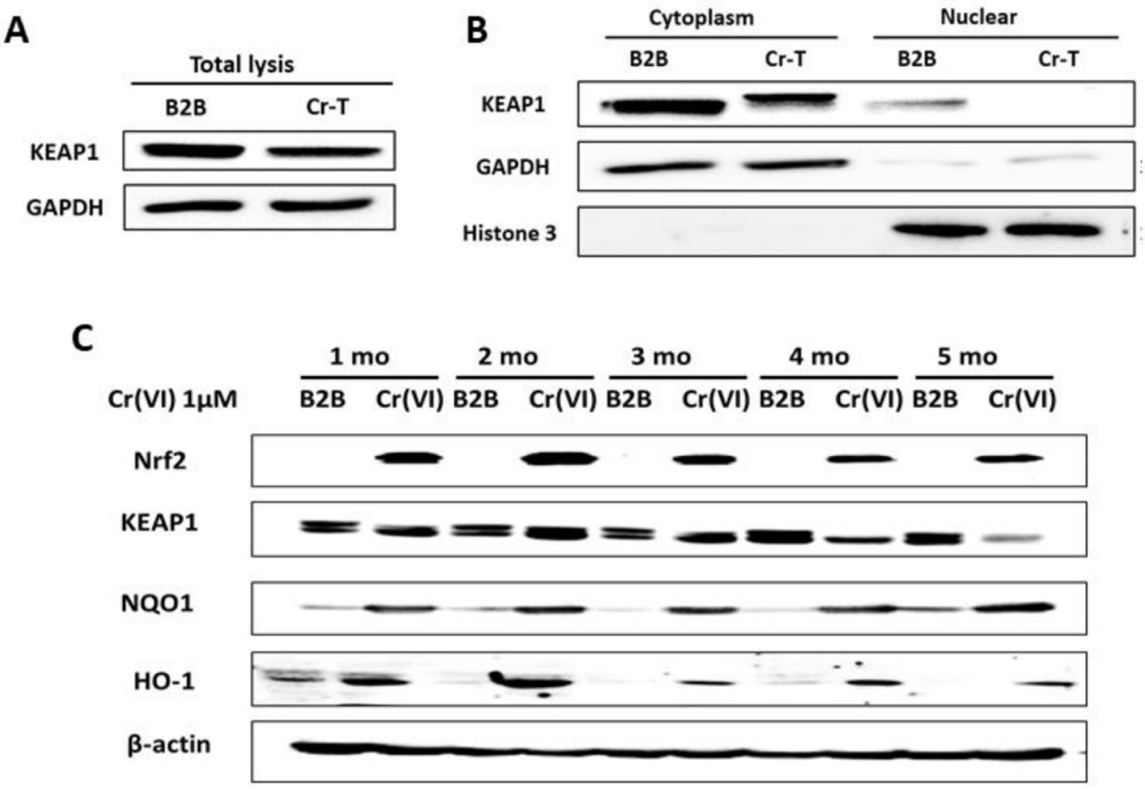

Fig. 2. Downregulation of KEAP1 was responsible for increased Nrf2 expression at late stage, but not at early stage of Cr(VI) exposure.

(**A**) Total lysates from Cr-T cells and parental B2B cells were used to test the expression of KEAP1 and β-actin using immunoblotting assay. (**B**) The expression of KEAP1 in cytoplasm and nuclear fraction. GAPDH and Histone 3 were used as an internal control for cytoplasm and nuclear fraction, respectively. (**C**) BEAS-2B cells were treated with 1 μM of Cr(VI) for different time points. The expression levels of Nrf2, KEAP1, NQO1, HO-1 and β-actin were analyzed using immunoblotting assay.

Author Manuscript Author Manuscript Author Manuscript Author Manuscript

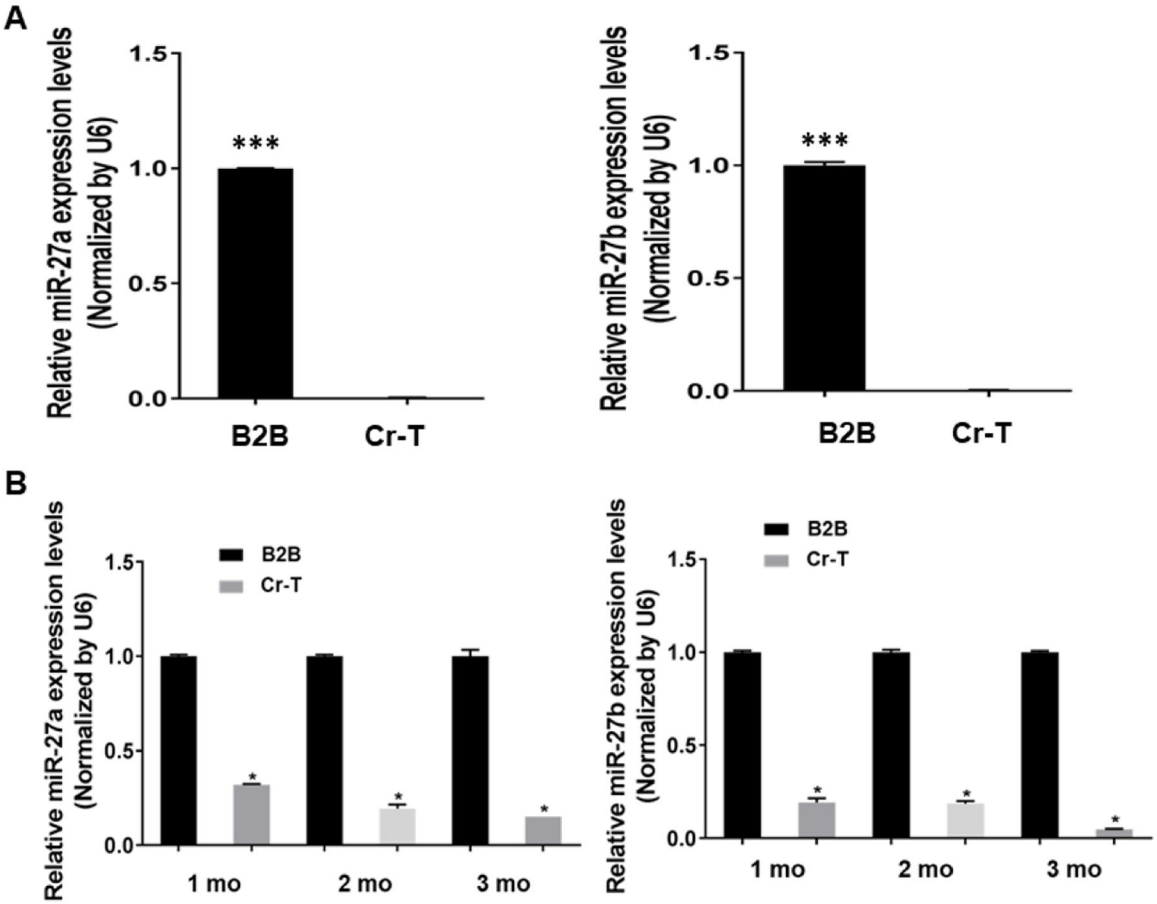

Author Manuscript Author Manuscript Author Manuscript Author Manuscript

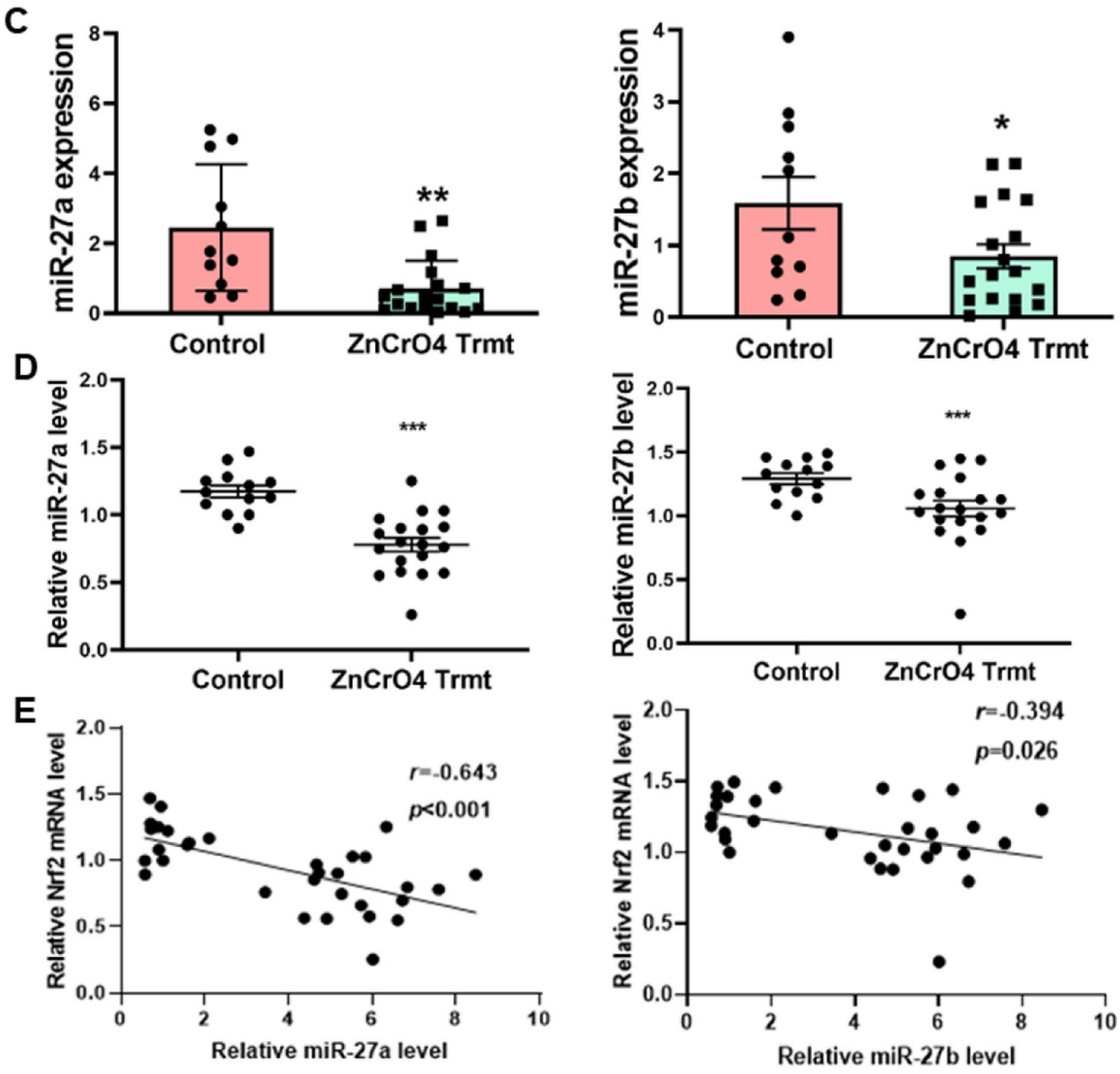

Fig 3. MiR-27a and miR-27b were downregulated upon long-term Cr(VI) exposure *in vitro* and *in vivo*.

(**A**) The mRNA levels of miR-27a and miR-27b in Cr-T and parental B2B cells were determined using TaqMan real-time PCR. (**B**) BEAS-2B cells were exposed to 1 μM of Cr(VI) for 1, 2 and 3 months. The expression of miR-27a/b were tested as above. (**C**) BALB/cJ mice were exposed to zinc chromate particles in sterile 0.9% sodium chloride solution at a concentration of 1.0 mg/ml for 12 weeks. MiR-27a/b levels were tested in peripheral blood mononuclear cells (PBMCs) in blood samples from Cr(VI)-exposed mice (n=18) and saline treatment control mice (n=11). (**D**) miR-27a/b expression in lung tissues from Cr(VI)-exposed mice (n=19) and saline treatment control mice (n=13). (**E**) The inverse correlation between miR-27a/b and Nrf2 expression in lung tissues (r=−0.643 and r=−0.394, respectively). *, $p < 0.05$, **, $p < 0.01$,***, $p < 0.0001$ compared to control group.

Author Manuscript Author Manuscript Author Manuscript Author Manuscript

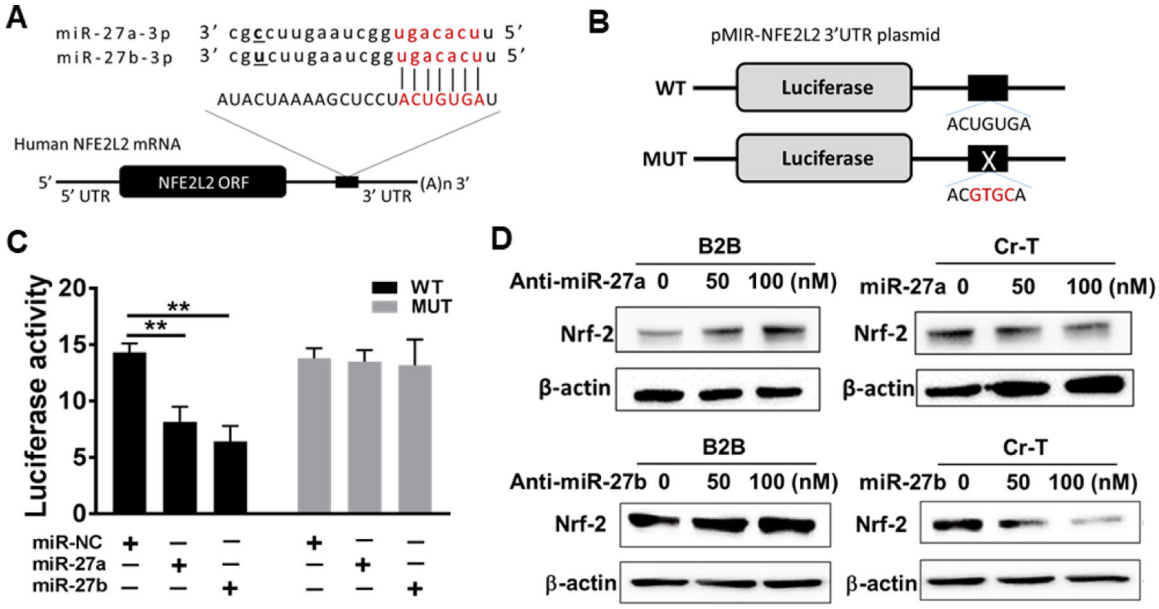

Fig 4. MiR-27a/b directly targeted Nrf2.

(**A**) Putative seed-matching site between miR-27a/b and 3'-UTR of Nrf2 (NFE2L2). (**B**) Diagram for wild type (WT) and mutant (Mut) luciferase reporter constructs. (**C**) Luciferase reporter assay was performed using Cr-T cells to detect the relative luciferase activities of WT and Mut Nrf2 reporters with or without miR-27a/b overexpression. Renilla luciferase vector was used as an internal control. Negative control of miRNA (miR-NC) was used as control for miR-27a/b transfection. **, $p < 0.01$ compared to control group. (**D**) BEAS-2B cells were transfected with anit-miR-27a/b at concentration of 50 nM and 100 nM, extracted proteins were subjected to Nrf2 and β-actin expression using immunoblotting assay. Similarly, Cr-T cells were treated with miR-27a/b mimics at concentration of 50 nM and 100 nM. miR-NC was used as control. Protein levels of Nrf2 and β-actin were analyzed using immunoblotting assay 72 h post transfection. Data were represented by means ±SE of triplicates.

Author Manuscript Author Manuscript Author Manuscript Author Manuscript

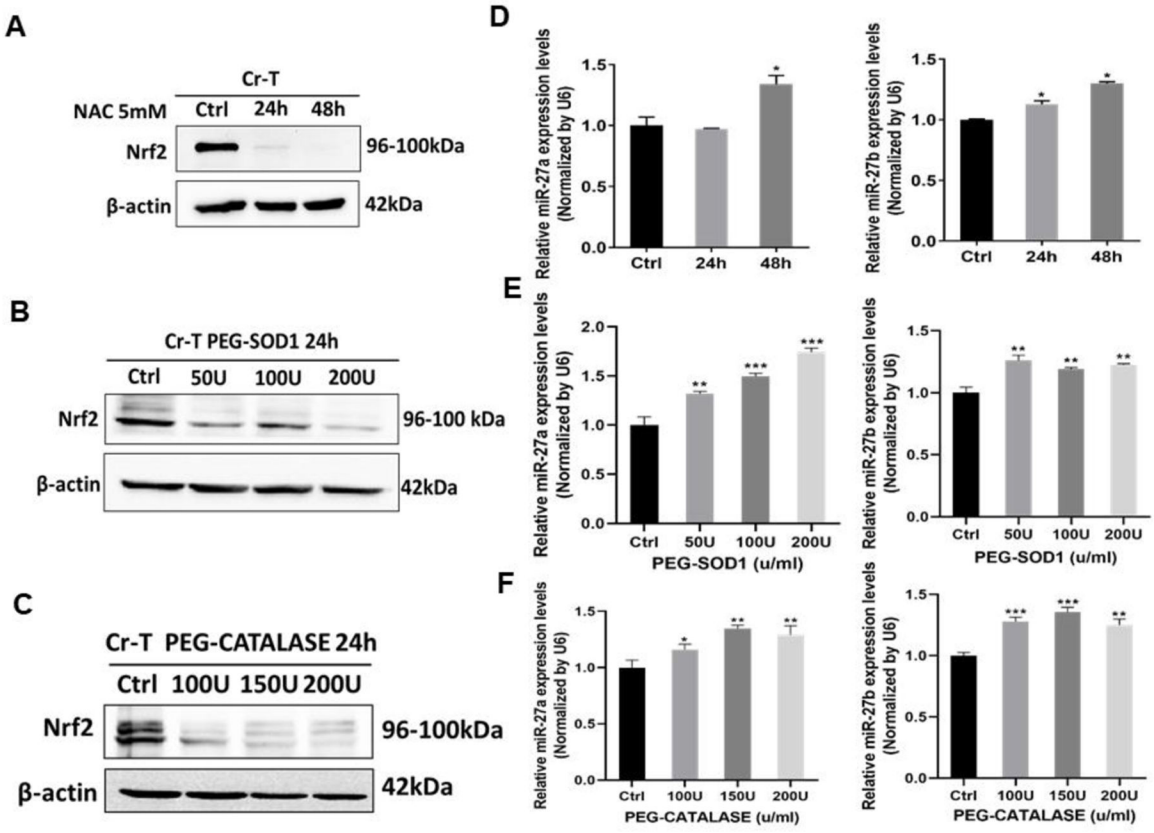

Fig 5. ROS-scavengers suppressed Nrf2 expression and restored miR-27a and miR-27b expression in Cr-T cells.

(**A**) Cr-T cells were treated with 5 mM of N-acetyl-I-cysteine (NAC) for 24 and 48 h. Solvent treatment was used as negative control. The expression of Nrf2 and β-actin was determined using immunoblotting assay. Cr-T cells were treated with 0, 50, 100 and 200U/ml PEG-SOD1 (**B**) or 0, 100, 150, and 200U/ml PEG-catalase (**C**) for 24 h. The expression of Nrf2 and β-actin was tested as above. (**D**) Cr-T cells were treated as Fig. 5A, miR-27a/b levels were analyzed using TaqMan real-time PCR method. (**E** and **F**) Cr-T cells were treated with PEG-SOD1 and PEG-catalase as above. The expression levels of miR-27a/b were tested using TaqMan real-time PCR. *, $p < 0.05$ compared to solvent control. **, $p < 0.01$ compared to solvent control. ***, $p < 0.001$ compared to solvent control.

Author Manuscript Author Manuscript Author Manuscript Author Manuscript

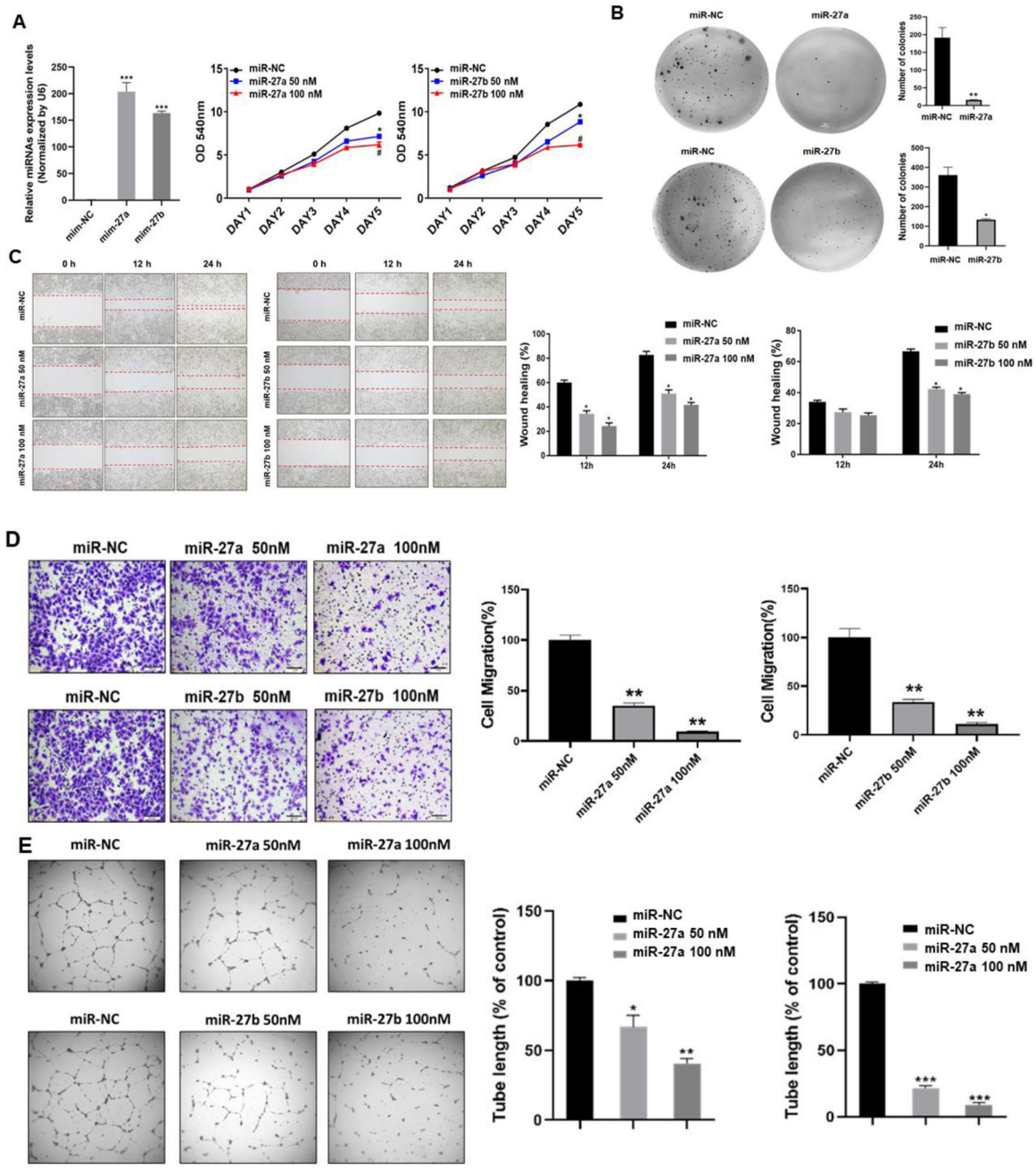

Fig 6. MiR-27a/b acted as tumor suppressors in Cr-T cells to inhibit cell proliferation, colony formation, migration and tube formation *in vitro*.

Cr-T cells were transfected with miR-27a, miR-27b or miR-NC. After 24 h, cells were trypsinized and seeded for cell proliferation assay using MTT method (**A**), colony formation assay using soft agar (**B**), wound healing assay (**C**), transwell migration assay (**D**), and tube formation assay (**E**). Quantitative results were shown using bar graph from three independent experiments. * and #, $p < 0.05$ compared to miR-NC group. **, $p < 0.01$ compared to miR-NC group. ***, $p < 0.001$ compared to miR-NC group.

Author Manuscript Author Manuscript Author Manuscript Author Manuscript

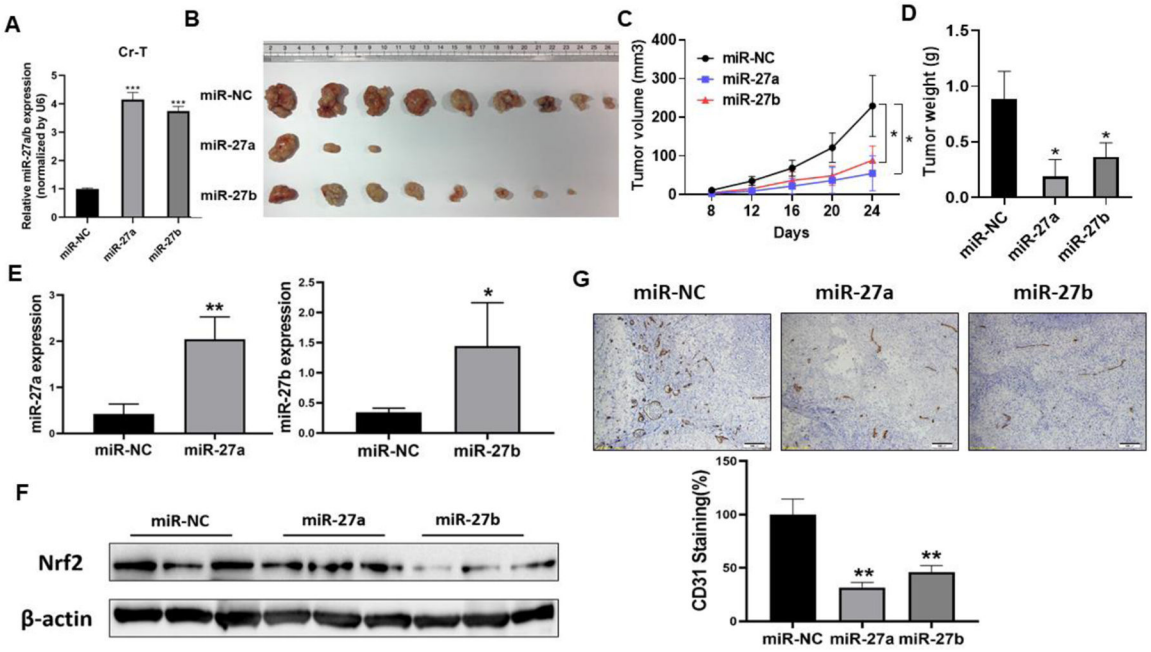

Fig 7. MiR-27a/b inhibited Cr-T cells-induced tumor formation and growth in nude mice.

(**A**) Establish Cr-T overexpressing miR-27a and miR-27b stable cells by lentiviral transduction and puromycin selection. The expression of miR-27a/b was determined by TaqMan real-time PCR. ***, $p < 0.0001$ compared to miR-NC stable cells. (**B**) miR-NC, miR-27a and miR-27b overexpressing Cr-T cells at $2x10^6$ were injected into flanks of 6-week old nude mice. Mice were euthanized and tumor xenografts were collected after 4 weeks of injection. The image showed representative tumors collected from each group. (**C**) Tumor size was measured twice per week when xenografts were visible. *, $p < 0.05$ compared to miR-NC group. (**D**) Tumor weight of miR-NC, miR-27a and miR-27b groups. *, $p < 0.05$ compared to miR-NC group. (**E**) Nrf2 expression from tumor tissues of miR-NC, miR-27a and miR-27b groups. (**F**) The expression levels of miR-27a and miR-27b from xenografts (n=3 for miR-27a group; n=5 for miR-NC and miR-27b groups). *, $p < 0.05$ compared to miR-NC group. **, $p < 0.01$ compared to miR-NC group. (**G**) CD31 positive microvessels. The number was normalized by miR-NC control group. **, $p < 0.01$ compared to miR-NC group.

Author Manuscript Author Manuscript Author Manuscript Author Manuscript

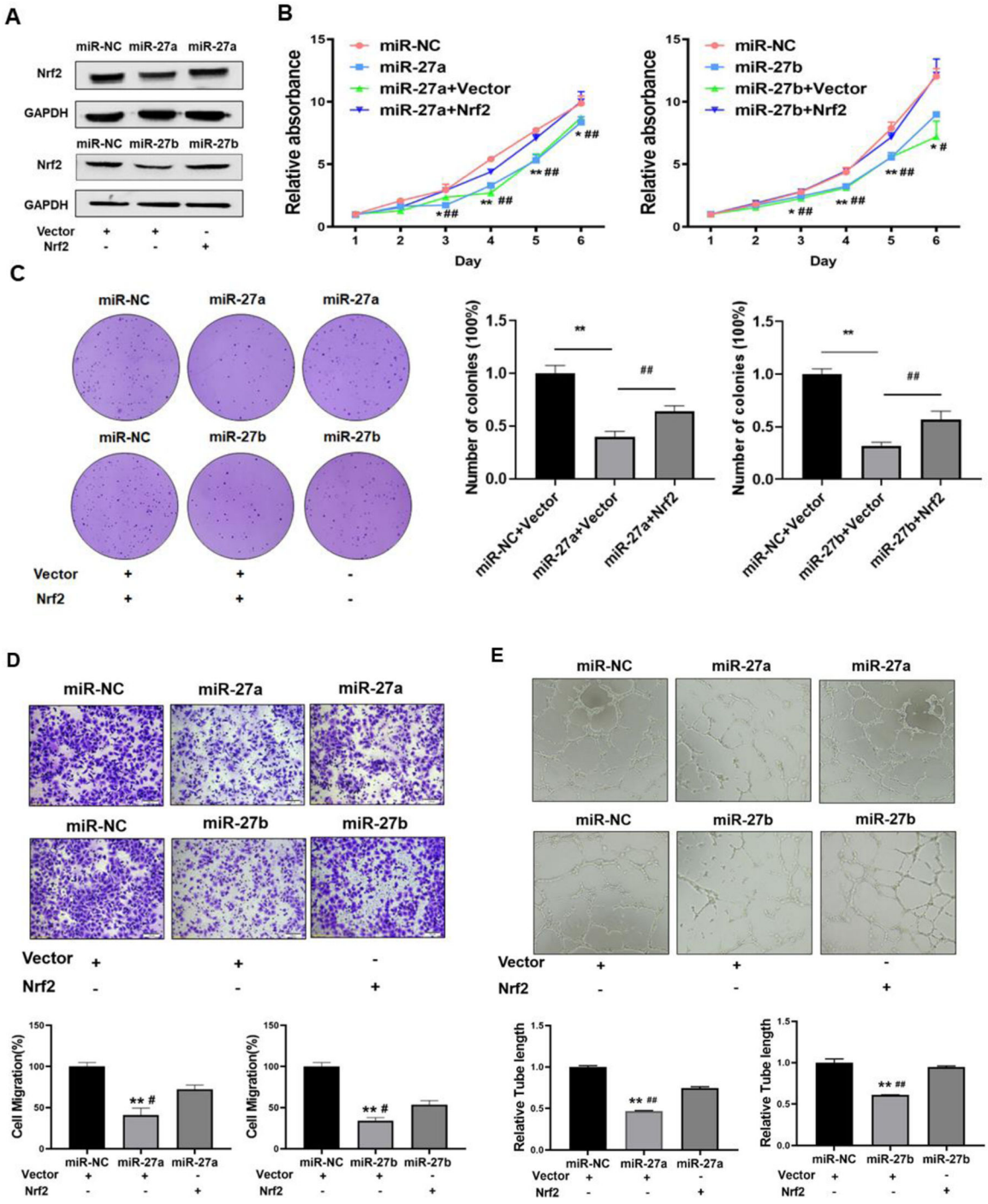

Fig 8. Forced expression of Nrf2 restored miR-27a/b-inhibited cell proliferation, colony formation, migration and tube formation.

Cr-T cells were transient transfected with miR-NC, miR-27a, miR-27b with vector control or Nrf2 ORF plasmid. (**A**) The expression of Nrf2 was analyzed 72 h after transfection using immunoblotting assay. After 24 h post transfection, cells were trypsinized and seed for cell proliferation assay using MTT method (**B**), colony formation assay using soft agar (**C**), transwell migration assay (**D**), and tube formation assay (**E**). Quantitative results were

shown using bar graph from three independent experiments. * and #, $p < 0.05$ compared to miR-NC group and miR-27a/b + Nrf2 group, respectively. ** and ##, $p < 0.01$ compared to miR-NC group and miR-27a/b + Nrf2 group, respectively.

Author Manuscript Author Manuscript Author Manuscript Author Manuscript

Author Manuscript

Author Manuscript

Author Manuscript

Author Manuscript

Table 1

Tumor growth assay in nude mice

Xenografts	Number of injections	Number of tumor formation
miR-NC	10	9
miR-27a	10	3
miR-27b	10	8